Lecture 25: Analysis of wedge fringes and Michelson interferograms

The Lecture Contains:

Previous Next

Wedge Fringe Interferograms

The Mach-Zehnder interferometer is not always used with the two interfering wavefronts parallel to each other, as in the infinite-fringe setting discussed above. There is a second mode in which the two interfering wavefronts have a small angle θ between them, introduced deliberately during alignment. Upon interference they produce an image consisting of bright and dark fringes, representing the loci of constructive and destructive interference respectively. These parallel and equally spaced fringes are referred to as wedge fringes. The spacing between the wedge fringes is a function of the tilt angle θ and the wavelength λ of the laser light used, and is given by

$$d = \frac{l/2}{\sin(q/2)}$$

For small tilt angles, the above expression becomes

$$d = \frac{l}{q}$$

As θ is decreased to zero, the wedge fringes get farther apart, approaching the infinite-fringe pattern.

When a thermal or concentration field is introduced in the path of the test beam, the phase of the test wavefront gets distorted depending upon the nature of the disturbance introduced. Upon interference with the reference wavefront, it manifests itself as a change from straight and parallel to curved fringes. The two interference patterns are shown schematically in Figure 4.67 below.

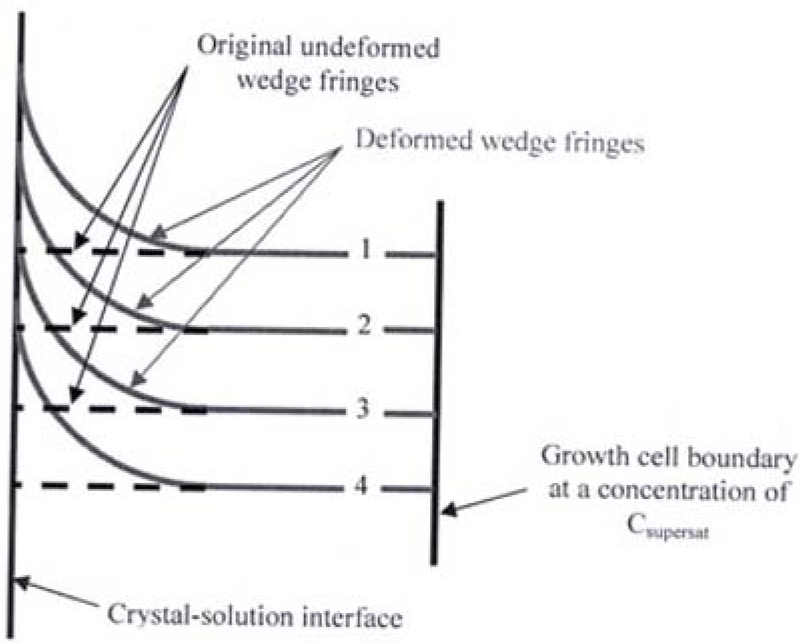

Figure 4.67: Wedge Fringe pattern with and without the field of disturbance

Figure 4.68 is an expanded view of the wedge fringes. Let us find concentration (of a solute in a solution or change in temperature from a reference value in a physical domain) at any point in the interferogram. The deviation of fringe 2 near the crystal-solution interface is D, while at any other point, it is denoted as d. Since fringe displacement relates linearly with change in phase, hence refractive index and material density, we can write

$$\frac{C\,(x) - C_{sat}}{C_{supersat} - C_{sat}} = \frac{d}{D}$$

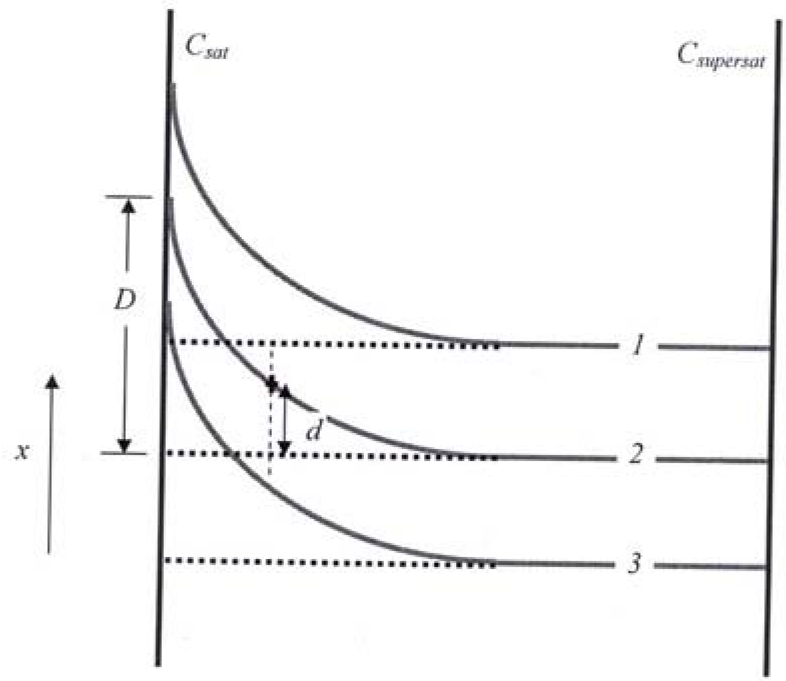

Figure 4.68: Computing concentration in the presence of the wedge fringes

Since all other parameters except $C(x)$ are known, the local concentration can be easily calculated. The concentration gradient dC/dx is obtained from the slope of the fringes at a point x. The above methodology is used for calculating the concentration at points which lie on the wedge fringes. However, if one were to find concentration at a point lying between two wedge fringes, instead of on them, then one has to locate four nearby points on the wedge fringes and compute their respective concentrations. It is then followed by using a suitable interpolation technique to find the concentration at the desired point.

Concentration data over a uniform grid

Once the absolute concentration corresponding to the fringes (in the wedge as well as infinite fringe setting) has been computed, the irregularly spaced concentration data must be transferred to a two-dimensional uniform grid over the fluid region. This is necessary to enable application of the tomographic algorithms for reconstruction of the three-dimensional concentration field. For this purpose, a two-dimensional linear interpolation procedure is followed by superimposing a 2D grid over the thinned interferograms. After completing the interpolation procedure, the equi-concentration contours are plotted. These contours should closely follow the originally recorded fringe pattern. It works as a cross-check for the data obtained after interpolation and provides an estimate of the interpolation errors.

Previous Next

Michelson interferometry

In a Michelson interferometer, the test beam and the reference beam develop a phase difference, not due to changes in refractive index along the path of light propagation but because of movement of one of the active surfaces. If the reference beam reflects off a fixed surface, the test beam, reflecting off a moving surface will interfere with the reference beam and produce an interference pattern. The simplest configuration of a Michelson interferometer is shown in Figure 4.68.

For definiteness, the application to Michelson interferometer to a crystal growth experiment is described below. Here, a seed crystal is immersed in its aqueous solution, supersaturated at the temperature considered. The excess salt deposits on the crystal introduced and the concerned surface grows with time. If this surface is taken as one off which the test beam is reflected, the growth rate can be monitored as a function of the position along the crystal and with time.

Consider a Michelson interferometer based experiment which is set-up for on-line monitoring of the microtopography of the growing face of a crystal. In this interferometry, one of the interfering beams is reflected from the surface of a growing crystal to get the microtopographic details of the growing surface. Since interferometry through the solution requires reflection of the light beam from the solution-crystal interface, it is a difficult task. Clear fringes can be recorded when the difference in refractive index between the solution and the crystal is sufficiently large. In spite of the inherent difficulties in working with this technique, it can be effectively used for studies in growth kinetics of crystals from their aqueous solution.

The basic principle of the Michelson interferometry in the context of crystal growth is that the phase variation due to growth or dissolution of the crystal surface manifests itself in the form of change in the fringe pattern. For example, if a crystal face has a growth hillock originating from a screw dislocation, the corresponding interference pattern consists of concentric fringes of equal thickness. Figure 4.68 shows schematically the process of fringe formation from a surface having a hillock generated from a dislocation. With every change in the crystal thickness by $\lambda/2n$, one fringe shift takes place. Here λ is the wavelength of the laser used, and *n* is the refractive index of the solution. From such an interferogram the geographical description of the crystal face is obtained. Quantitative analysis of the interferogram yields the growth-kinetic parameters such as normal growth rate R, slope of the dislocation growth hillock p, and tangential growth velocity V of the steps.

Contd...

These are computed as follows:

The difference of heights between two points on adjacent fringes of an interferogram corresponding to a growth hillock or dissolution valley is given by

$$d = \frac{\lambda}{2n}$$

If the total variation in the crystal thickness normal to the crystal face is Δh in time Δt, the normal average growth rate is given by

$$R = \frac{\Delta h}{\Delta t}$$

where $\Delta h = N \times d$. The symbol N is the total number of fringes that have crossed the point of observation on the interferogram. Thus the normal average growth rate becomes

$$R = \frac{N \times \lambda}{2 \times n \times \Delta t}$$

If D is the physical distance between the two points lying on adjacent fringes, the slope p of the hillock is given by

$$p = tan\theta = \frac{d}{D}$$

The normal growth rate and the slope of the dislocation hillock are related to the tangential step velocity V as follows:

$$R = p \times V$$

Thus by calculating R and p, the tangential step velocity V is obtained.

Previous Next

Module 4: Interferometry

Lecture 25: Analysis of wedge fringes and Michelson interferograms

Michelson interferograms provide direct visual evidence of the mechanism of growth, e.g. spiral growth, two-dimensional nucleation, or birth-and-spread growth. Initially the interferometer is aligned with wedge fringes, which are then separated to yield the infinite-fringe interferogram. Under this setting the minute micro-morphological details become visible. They indicate the growth mechanism by which a particular face grows with time. These features are observed in-situ and in real time.

Sample images recorded in a crystal growth experiment by the Michelson interferometer are shown in Figure 4.69.

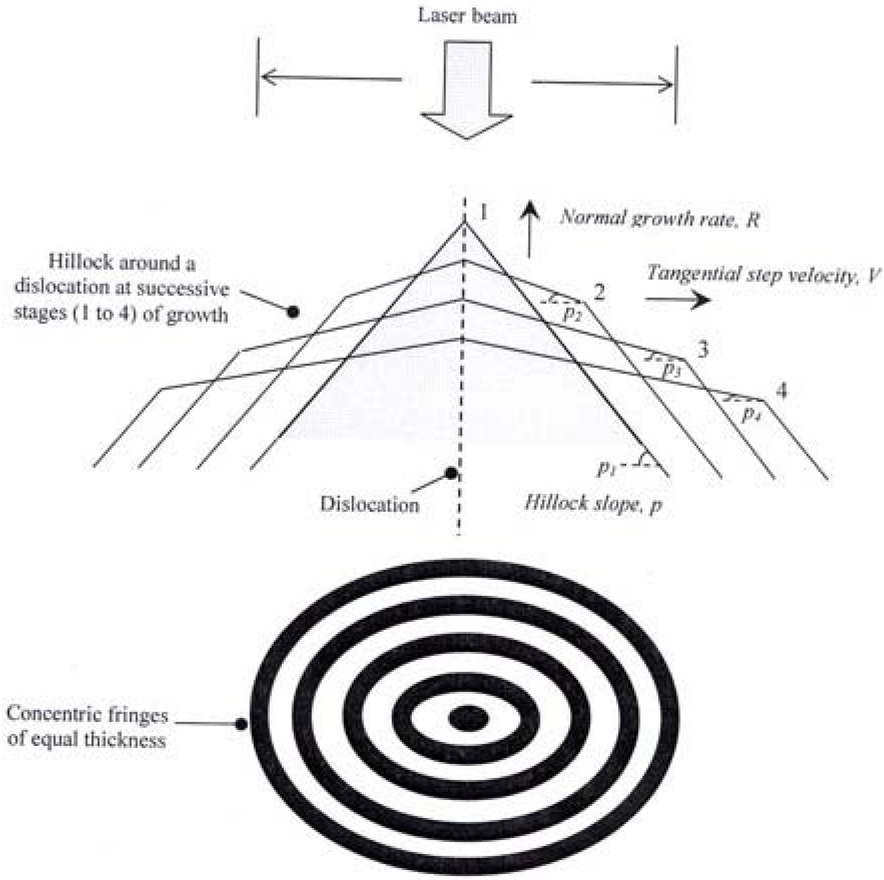

Figure 4.69: Schematic drawing of the Michelson Fringe formation from a crystal face having a hillock generated from a dislocation

Previous Next

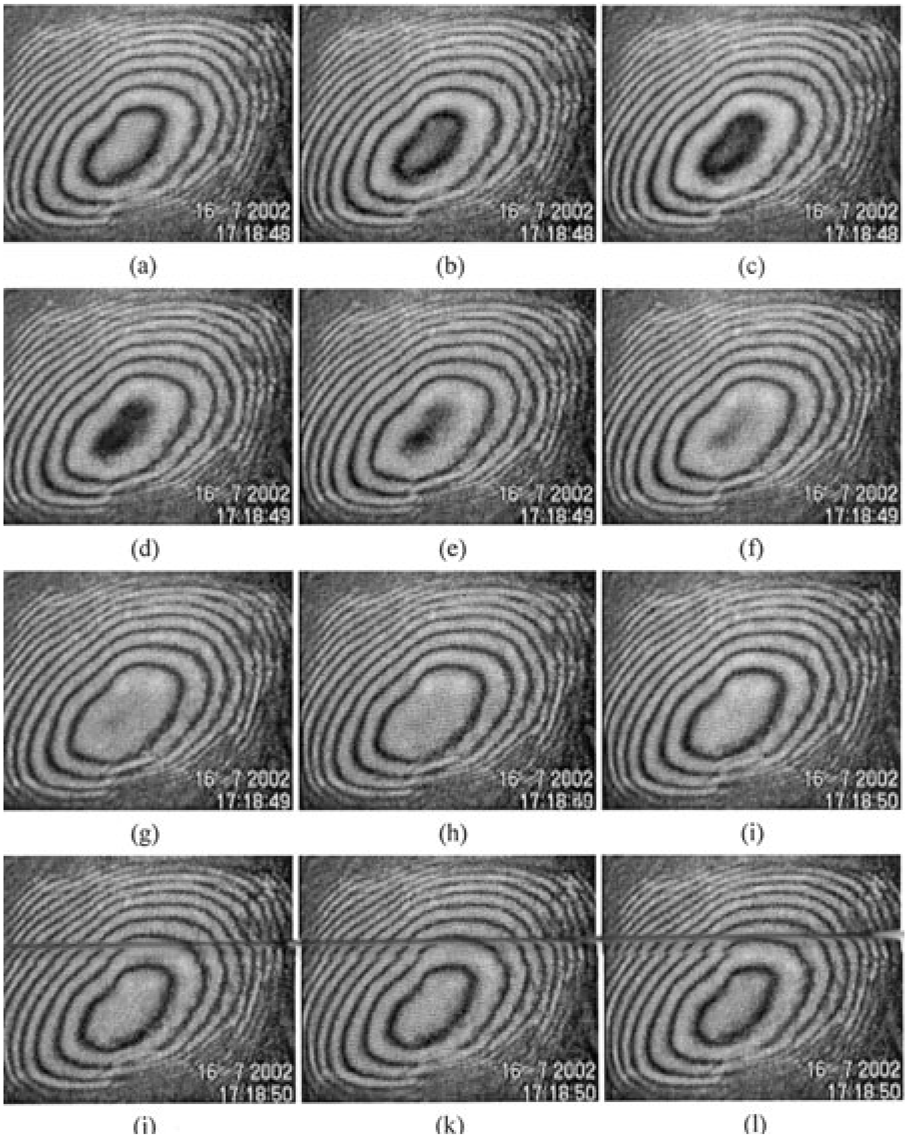

Figure 4.70(a-l): Time sequence of Michelson interferograms showing fractional movement (inwards) of one complete fringe during dissolution of the KDP crystal by heating of the aqueous solution.

Michelson cum Mach-Zehnder interferometer

Another optical schematic comprising a Michelson and a Mach-Zehnder interferometer into a single set up is proposed for simultaneous studies described above. The combined interferometer is shown in Figure 4.71. The incoming laser beam is split into two beams using a beam splitter. In order to get the surface structure details, the two beams split by the first beam splitter (BS1) are used along with an optical glass window (W) to form a Michelson interferometer. Under normal incidence, approximately 4% light intensity is reflected from the front surface of the glass window. This reflected beam from the window becomes the reference beam of the Michelson interferometer and interferes with a second beam that is obtained after reflection from the crystal surface. This results in a Michelson interferogram that carries the microstructure details of the growing crystal surface. In order to obtain solution characteristics, the two beams split by the first beam splitter (BS1) are used again. These are folded using mirrors (M1 and M2) and beam-splitters (BS1 and BS2) placed at the corners of a rectangle to form a Mach-Zehnder interferometer. The 96% intensity of the reference beam that gets transmitted through the glass window used for the Michelson interferometer interferes with the beam that passes through the chamber where the crystal is growing. The interference of these two beams yields a Mach-Zehnder interferogram that carries details of the thermal, concentration and convective field around the growing crystal. In this manner two interferograms are obtained simultaneously on two CCD cameras to result in the microtopography as well as transport characteristics during growth.

Previous Next

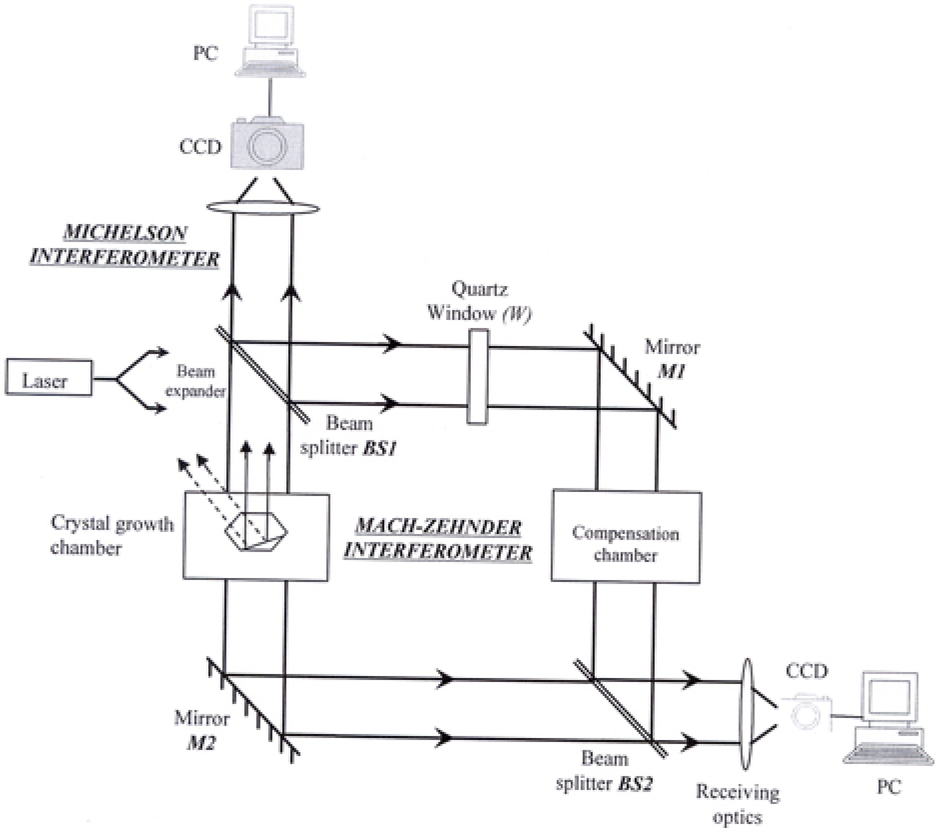

Figure 4.71: Optical layout of a combined Michelson and Mach-Zehnder Interferometer

Previous Next